EXPERIMENTAL INVESTIGATION ON THE BEHAVIOUR OF HYBRID HPFRC FLAT SLABS

Brisid Isufi [1,*], Carla Marchão [1], Rui Marreiros [1], António Pinho Ramos[1,2]

1. DEC, NOVA School of Science and Technology, UNL, Caparica, Portugal
2. CERIS, Lisbon, Portugal

[*]Corresponding author email: b.isufi@campus.fct.unl.pt

ABSTRACT

Reinforced concrete flat slabs is a widespread structural solution in office, commercial and residential buildings around the world. Punching shear often governs the design of these structures, leading to increased self-weight and material consumption when thickness increase is sought as a solution or increased labor costs in the case of punching shear reinforcement utilization. New possibilities are arising with the development of advanced concrete materials such as High-Performance Fiber Reinforced Concrete (HPFRC) to improve the behavior of flat slabs subjected to punching shear. HPFRC offers the advantages of both High Strength Concrete (HSC) and Fiber Reinforced Concrete (FRC) as well as an increased performance in terms of self-compactness and durability. Motivated by the scarcity of previous experimental research on slabs with realistic thickness and the promising results obtained in the past from specimens with FRC and HSC, this paper describes an experimental program with the aim of studying the behavior of HPFRC flat slabs under monotonic punching loading. To study the possibility of minimizing HPFRC consumption, the specimens were designed and produced as hybrid specimens, with HPFRC used only in the vicinity of the support column, being the rest of the slab casted with a Normal Strength Concrete (NSC). The experimental variables were the flexural reinforcement ratio (0.6% and 1.0%) and the extent of the HPFRC zone (1.5 and 3.0 times the effective depth of the slab, measured from the face of the column). A total of five specimens were tested, including a NSC reference specimen. The results show that HPFRC applied over a limited region near the column can increase the cracking load, maximum load carrying capacity as well as the displacement at failure. These benefits are apparent even with a small extent of the HPFRC zone (only 1.5 times the effective depth from the face of the column).

Keywords: flat slab; flat plate; punching; shear; HPFRC; high performance fiber reinforced concrete

INTRODUCTION

Punching shear failure is often the governing failure mode in flat slabs. Potential solutions to increase punching shear strength include the increase of slab's thickness (either across the entire floor or only in the vicinity of the column, in the form of a drop panel) or the provision of punching shear reinforcement. The former leads to an increase in the consumption of raw materials by the increase of the volume of concrete, but also indirectly due to the increased weight and mass of the building that leads to increased demands for the entire structure. The latter has been shown to be very effective in increasing punching shear strength of flat slabs, but it is often labor intensive, prone to execution errors, and sometimes leads to a congestion of reinforcement near the column that complicates concrete casting. In addition to punching shear, serviceability design often governs the design of reinforced concrete flat slabs, and the adoption of punching shear reinforcement cannot mitigate these issues.

With the development of concrete technology and the advent of advanced concrete materials such as High Strength Concrete (HSC) and Fiber Reinforced Concrete (FRC), new possibilities have arisen to minimize the aforementioned problems in flat slabs and reduce the overall consumption of materials and/or labor costs. Significant research on the use of advanced concrete materials to mitigate punching shear issues in flat slabs started in the 1980s' and early 1990s' with works from Swamy and Ali [1], Narayanan and Darwish [2] on FRC and Marzouk and Hussein [3] on HSC, although previous works

on small scale specimens also exist. Early studies showed that the use of HSC and FRC has great potential to increase punching shear strength and the overall performance of flat slabs subjected to gravity loading.

One of the main conclusions of the detailed literature review on the application of HSC and FRC in flat slabs, that can be found in Isufi and Ramos [4], is that the combination of HSC with FRC has not been sufficiently explored in flat slabs. Such a combination is potentially beneficial for flat slabs subjected to punching shear because the high strength of concrete can lead to an increased punching shear strength, whereas steel fibers can reduce and control internal cracking, both leading to an increase of punching shear capacity. Experimental studies that have investigated this possibility in the past include Chanthabouala et al. [5], in which a FRC with compressive strength above 80 MPa was used in 150 mm thick slabs tested under gravity loading, and Ozden et al. [6] that tested 120 mm thick circular slabs with 1.5m diameter. In addition, tests on small scale slabs (thickness below 100 mm) can also be found in the literature.

The present study investigates the behavior of large-scale composite slabs under punching shear with hybrid use of Normal Strength Concrete (NSC) and high-strength fiber reinforced concrete. Due to the specifics of the later, which are not only related to compressive strength but also to performance in general (durability, tensile behavior, self-compacting properties), this material is called High Performance Fiber Reinforced Concrete (HPFRC) from here on. To take full advantage of its characteristics and to balance its high cost, the hybrid use of HPFRC in this research aims to reduce its quantity, and it is motivated by past research on HSC slabs [7,8], FRC slabs [1,9–11] and Ultrahigh-Performance Concrete (UHPC) slabs [12].

DESCRIPTION OF HPFRC

The HPFRC used in this research was developed by Nunes et al. [13] and presented also in Blazy et al. [14]. The mix design is shown in Table 1. The mixture includes two types of steel fibers (hybrid mixture): triple hooked-end long fibers with 0.9 mm diameter and 60 mm length and straight fibers with 0.2 mm diameter and 13 mm length, with a volume fraction V_f = 1% (0.5% corresponding to the long fibers and 0.5% to the short fibers). This mixture was chosen after an extensive experimental campaign described in [13], that showed that the binary mixture used in this study had the best performance (highest crack mouth opening displacement at maximum load in a wedge-splitting test and good self-compacting properties).

Table 1 – Mix proportions of the HPFRC

Material	Quantity (kg/m^3)
Cement CEM I 42.5R	531.86
Limestone powder	203.72
Silica fume	53.19
Water	147.85
Superplasticizer	12.55
Fine aggregates	811.82
Coarse aggregates	721.43
Steel fibers (long)	39.25
Steel fibers (short)	39.25

Based on [13], where detailed material characterization is provided, the developed HPFRC presents a compressive strength for 150-mm width cubes of about 125 MPa and for 150 mm diameter and 300 mm high cylinder of 114 MPa at 28 days. The flexural behavior is characterized by a stress at the limit of proportionality f_L = 10 MPa and residual flexural tensile strengths f_{R1} = 15.4 MPa (for crack mouth opening displacement – CMOD – in a three-point bending test of 0.5 mm), f_{R2} = 18.0 MPa (for CMOD =1.5 mm), f_{R3} = 16.4 MPa (for CMOD = 2.5 mm) and f_{R4} = 12.9 MPa (for CMOD = 3.5 mm) [13]. It should be noted that f_L and f_{R1} to f_{R4} values are average values.

EXPERIMENTAL PROGRAM

Description of the specimens

Five specimens were produced and tested under monotonic punching loading. All specimens had a thickness of 150 mm, and an octagonal shape with overall dimensions of 2.2 m by 2.2 m (Fig. 1). The main experimental variables were the flexural reinforcement ratio ρ_l (0.6% and 1.0%) and the size of the HPFRC zone (600 mm square or 960 mm square) that corresponded to an extent ranging from 1.5d to 3.0d from the face of the column, where d is the average effective depth of the top reinforcement. As illustrated in Fig. 1, two specimens with different sizes of the HPFRC zone were cast for each flexural reinforcement ratio. For ρ_l = 0.6%, an additional reference specimen (without HPFRC) was cast. A corresponding reference specimen for ρ_l = 1.0% was not produced, because it was already tested in a previous research.

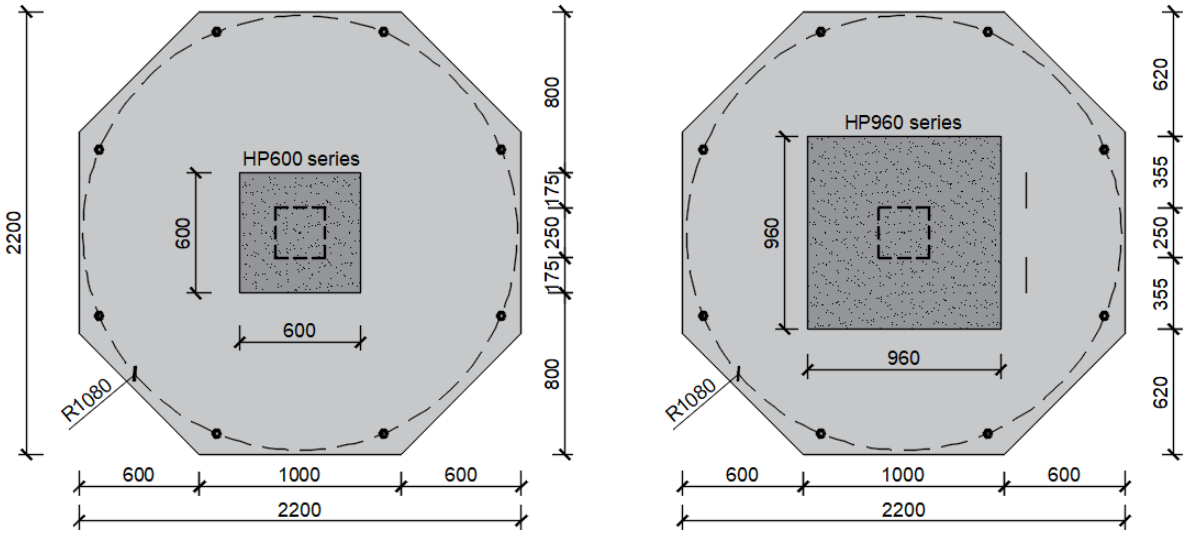

Figure 1 – Geometry of the specimens (units: mm)

The specimens were named using this convention: "HP" (representing HPFRC) followed by the width of the HPFRC zone (in millimeters), followed by an underscore and the letter "R" (for reinforcement) followed by the flexural reinforcement ratio (as a percentage). For example, specimen HP960_R0.6 is a specimen with a 960 mm square region with HPFRC and flexural reinforcement ratio of 0.6%.

For all specimens, 12 and 10 mm diameter deformed rebars were used for the top and bottom reinforcement meshes, respectively, as shown in Fig. 2. As usually adopted in the detailing of flat slabs, the spacing of top rebars near the column (up to roughly 3 times the effective depth from the face of the column) was smaller compared to the outer region. The specified nominal concrete cover was 20 mm. Table 2 presents the exact effective depth, d of the top bars measured right before casting, the average top flexural reinforcement ratios ρ_l (calculated based on Eurocode 2 [15]) and the width of the HPFRC zone expressed in value and as a multiple of d from the face of the column.

Table 2 – Characteristics of the specimens

Specimen	d (mm)	ρ_l (%)	HPFRC width c_{hpfrc} (mm)	HPFRC extent (d)
HP0_R0.6	117.7	0.64	0	0d
HP600_R0.6	118.4	0.64	600	1.5d
HP960_R0.6	118.0	0.64	960	3.0d
HP600_R1.0	117.5	0.96	600	1.5d
HP960_R1.0	117.9	0.96	960	3.0d

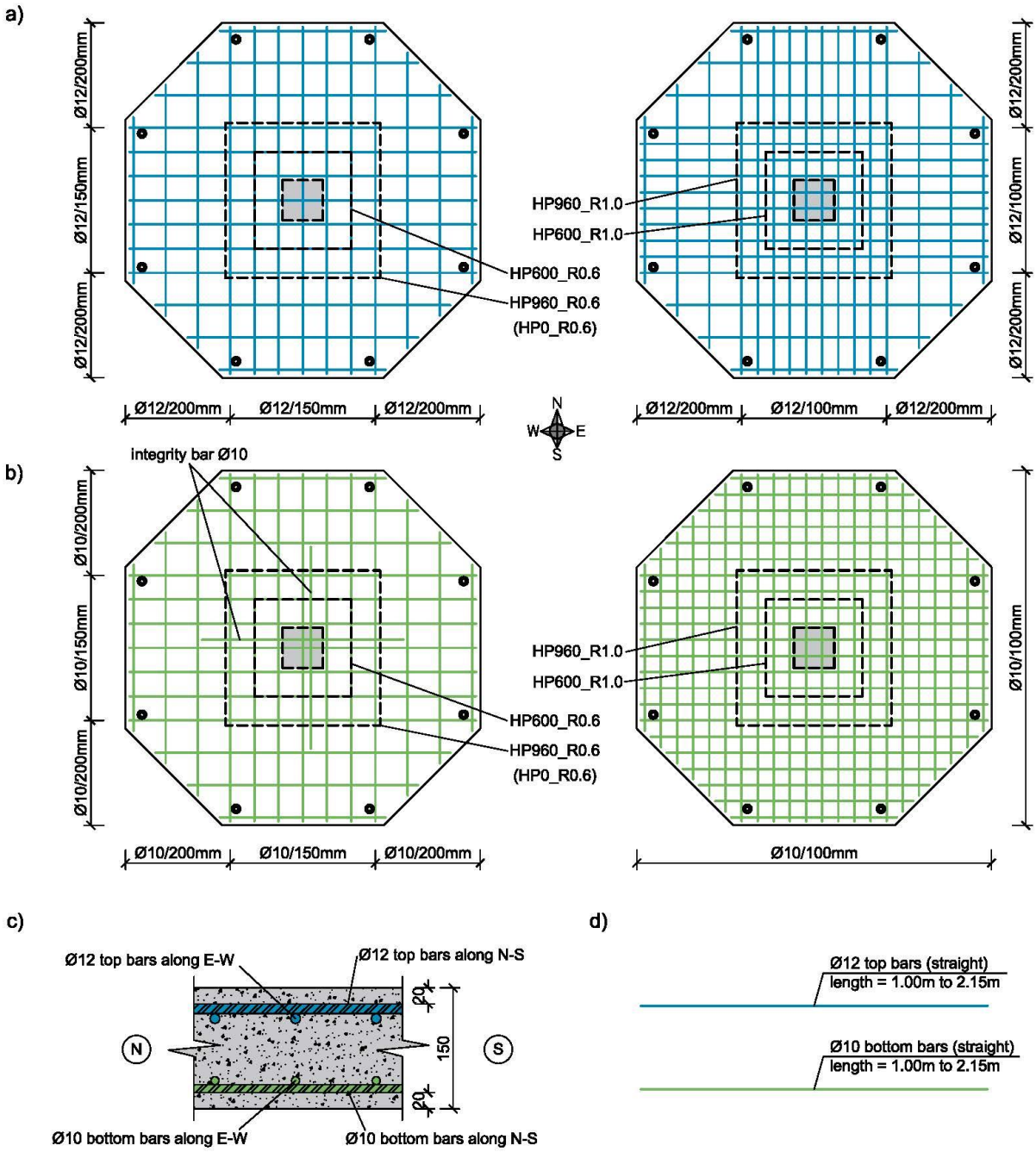

Figure 2 – Flexural reinforcement: a) top rebars; b) bottom rebars; c) cross-section detail; d) reinforcement detail

The specimens were cast-in-place on a plywood panel formwork that was prepared near the testing facilities at Nova School of Science and Technology (Fig. 3). To cast the specimens with different concretes (NSC and HPFRC), it was necessary to use a general-purpose fine galvanized steel mesh (diameter 0.5 mm and square shaped, with size 13 mm) at the interface between the two zones, connected to the top and bottom reinforcement bars. Considering the properties of HPFRC, namely its self-compacting properties as well as the relatively short setting time, it was decided to cast the outer region first (conventional concrete) followed by the HPFRC soon after (Fig. 3). After casting, the specimens were covered using a wet geotextile membrane and a plastic sheet for at least 7 days to prevent excessive water loss due to evaporation.

(a) (b)

Figure 3 – Casting of specimens: a) formwork and steel net; b) finished product

Test setup and instrumentation

The specimens represent the hogging moment region of a flat slab with equal spans in both orthogonal directions, supported on 250 mm square columns. The test setup is shown in Fig. 4. A central hydraulic jack with 1000 kN capacity and a maximum stroke of 153 mm was used to apply the load at a rate of approximately 150 N/s. The slab specimen was connected to the laboratory strong floor using a system of four spreader beams and eight strands as illustrated in Fig. 4. To measure the applied load throughout the test, eight load cells were installed on top of the slab at the locations of the strands, along the perimeter of the specimen. Eleven displacement transducers were installed on top of the slab and five additional ones were installed on the bottom surface, as shown in Fig. 5.

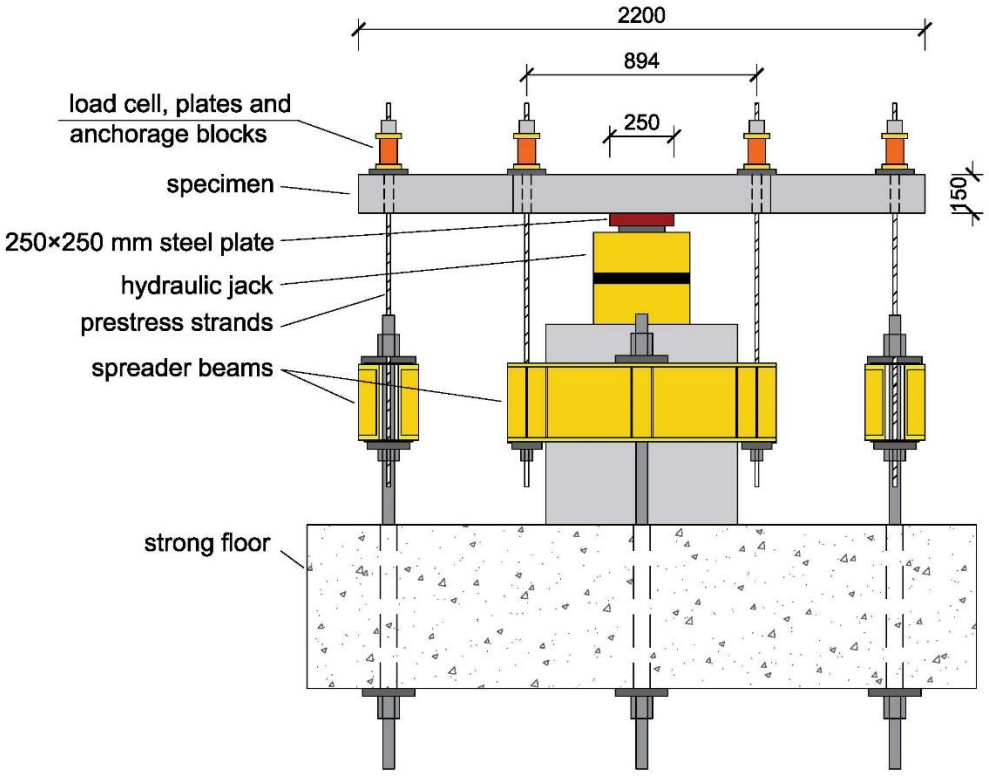

Figure 4 – Test setup (units: mm)

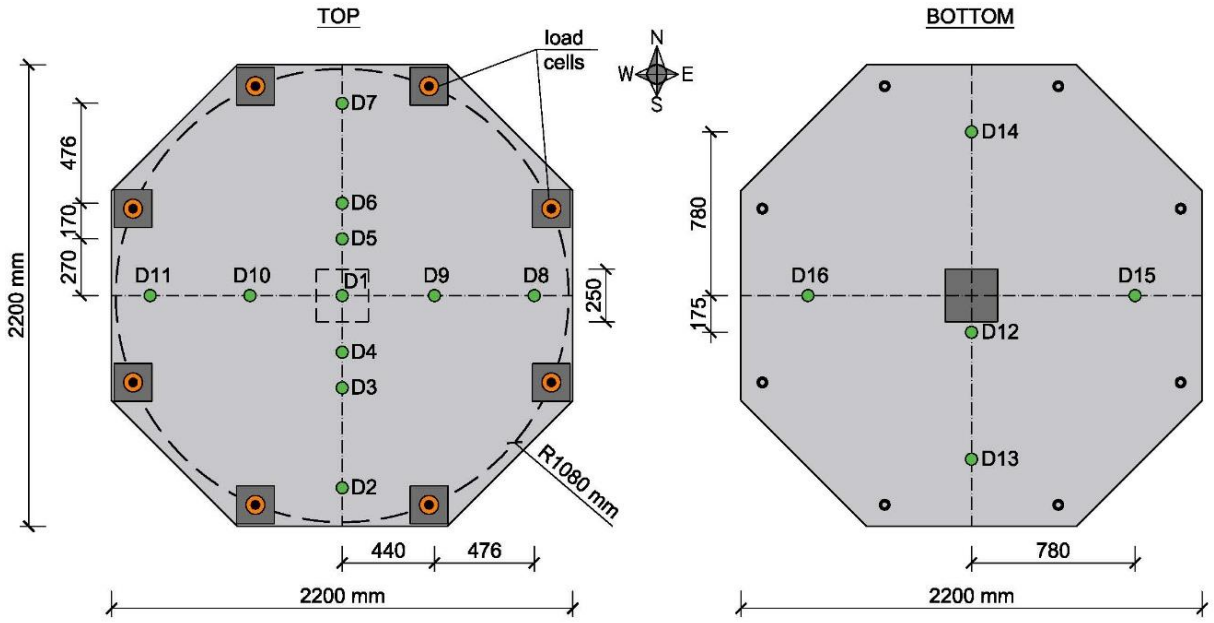

Figure 5 – Instrumentation: load cells and displacement transducers (units: mm)

Materials

Standard cubes (150 mm width) and cylinders (150 mm diameter, 300 mm high) from the NSC were tested in compression for each slab specimen to determine the compressive strengths $f_{c,cube}$ and f_c respectively. Prior to crushing, the cylinders were used to measure the modulus of elasticity, E. The tensile splitting strength of conventional concrete, $f_{ct,\,sp}$ was obtained by tensile splitting tests of three cylinders for each slab.

A detailed characterization of the developed HPFRC has been presented in earlier works [13,14]. To check compliance with previous tests, 100 mm cubes, 150 mm cubes and standard cylinders were cast for each slab. The 100 mm cubes were used in specimens where the compressive resistance of 150 mm cubes exceeded the operational capacity of the testing machine. The concrete properties for each specimen at the date of the tests are summarized in Table 3.

Table 3 – Concrete mechanical properties

Specimen	Conventional concrete				HPFRC			
	$f_{c,cube150}$ (MPa)	f_c (MPa)	$f_{ct,sp}$ (MPa)	E (GPa)	$f_{c,cube150}$ (MPa)	$f_{c,cube100}$ (MPa)	f_c (MPa)	E (GPa)
HP0_R0.6	25.4	24.4	2.2	29.0	N/A*	N/A	N/A	N/A
HP600_R0.6	25.2	27.5	2.2	29.5	120.0	N/A	126.1	51.5
HP960_R0.6	30.1	26.0	2.5	27.5	129.5	130.1	127.7	49.7
HP600_R1.0	28.1	24.6	2.2	25.1	N/A	126.6	123.9	49.3
HP960_R1.0	23.8	25.5	2.3	25.6	N/A	124.0	118.1	N/A

*not applicable, or not available

The steel reinforcement used for both layers of reinforcement consisted of deformed rebars. For the top bars, the yield strength was f_y = 547 MPa and the ultimate strength was f_u = 642 MPa.

EXPERIMENTAL RESULTS

Cracking and failure modes

The reference specimen (HP0_R0.6) showed a typical development of cracking throughout the test for flat slabs subjected to punching loads: radial flexural cracks appeared after the cracking load (about 60 kN) and grew steadily throughout the test. With the increase of the load, new cracks were formed on the top surface and the existing ones grew. The bottom surface suffered no noticeable damage until

punching shear occurred, characterized by an intrusion of the steel plate support into the slab. The saw-cut for this specimen shows a typical punching shear failure (Fig. 6).
For all specimens with HPFRC, cracking was delayed compared to the reference specimen HP0_R0.6, but after the appearance of the first crack, the development of the new cracks was similar for all. Regarding cracks that were detected, some remained only within the HPFRC zone, others crossed the HPFRC central region and extended towards the edges of the specimen. As expected, the specimens with lower flexural reinforcement ratio presented more cracks for the same level of loading. The bottom surface of specimens with HPFRC did not suffer any visible damage until very close to failure.

In specimen HP600_R0.6, a shear failure outside the HPFRC zone started on one side of the HPFRC square zone. Due to likely redistribution of the load after the beginning of this failure, crushing of the bottom surface of the specimen occurred along NW – SE direction before propagation of the shear failure around the perimeter of the HPFRC region. The failure line on the bottom surface crossed even the HPFRC region, with a deviation caused by the presence of the support. The saw-cuts presented in Fig. 6 provide additional insight about failure of HP600_R0.6. Near the reinforcement bar on the north side, failure crossed the HPFRC zone, whereas at other angles failure varied from shear failure outside the HPFRC zone to a combination of flexural damage and shear cracking.

Significant flexural cracks developed in HP960_R0.6 within the HPFRC region before failure. A premature punching shear failure occurred at one of the supports in the perimeter of the specimen at a load level that exceeded that of the similar specimen but with a smaller HPFRC region (HP600_R0.6). The saw-cut of Fig. 7 shows that there was a significant shear crack on the north side within the HPFRC zone, indicating that the specimen was close to failure. The crack was effectively controlled by the steel fibers, whereas cracking outside the HPFRC zone weakened the support region and likely caused failure at the border of the specimen.

In the two specimens with higher flexural reinforcement ratio (HP600_R1.0 and HP960_R1.0) eight steel plates were added under the load cells to prevent failures at the border of the specimens. Shear failure occurred outside the HPFRC region. In the specimen with smaller width of the HPFRC region, failure affected three sides of the outer perimeter of the HPFRC zone. Delamination of the concrete cover is visible on the top surface, on three sides of the perimeter, in similarity with a typical punching shear failure with a large perimeter. The failure perimeter was not closed (failure extended on three sides of the column when the test was stopped). In contrast to HP600_R0.6, the saw-cut (Fig. 6) shows that failure within HPFRC was not detected in HP600_R1.0.

In HP960_R1.0, the redistribution capacity of the shear force along the perimeter outside the HPFRC zone was even more limited due to the large perimeter of the HPFRC zone. This led to a shear failure resembling one-way shear in this specimen. However, the saw-cut (Fig. 6) along the N-S direction (along which the bars had higher effective depth) shows that a shear crack had developed also on the south side, opposite to the side in which visible failure occurred, that led to the end of the test.

In addition, the saw-cuts presented in Fig. 6 show that the solution used for the interface between the HPFRC and the NSC was efficient, showing a good bond behavior between the two different concretes. Minor imperfections occurred at the bottom part of the HPFRC zone in some specimens due to the vibration of conventional concrete which led to some intrusion of the NSC into the zone that was supposed to be cast with HPFRC.

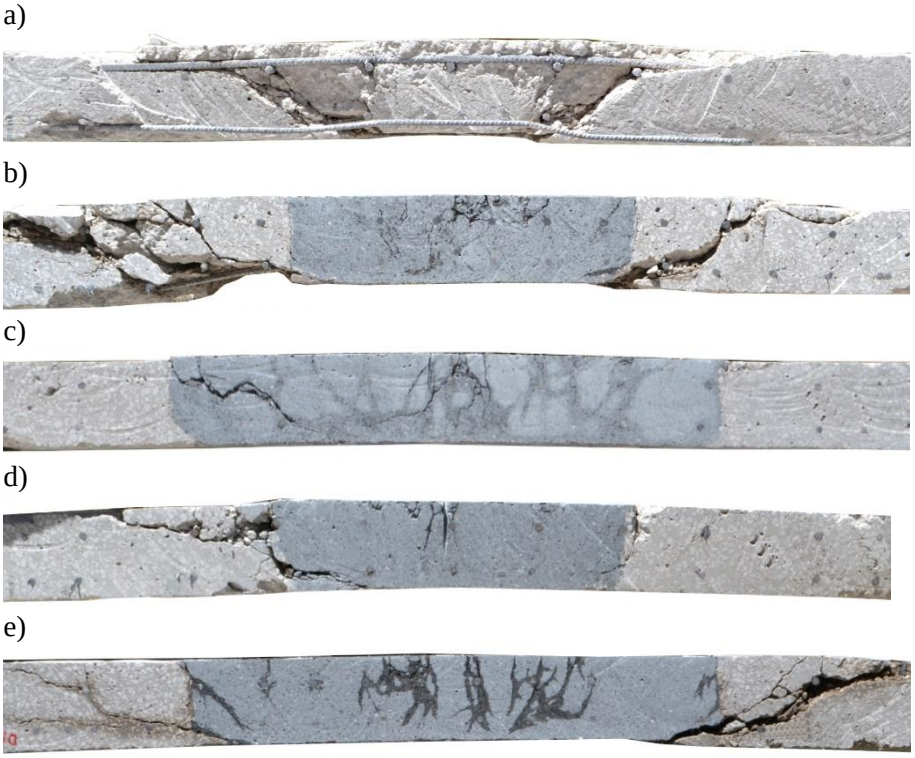

Fig. 6 – Saw-cuts of the specimens along N-S direction: a) HP0_R0.6; b) HP600_R0.6; c) HP960_R0.6; d) HP600_R1.0; e) HP960_R1.0

Load – displacement relationships

Fig. 7 presents the load (V) – displacement (u) curves for all specimens, comparing each set of HPFRC specimens with their respective reference specimen with NSC. It should be noted that the reference specimen F0_R1.0, previously published in Gouveia et al. [9], was nominally identical to specimens HP600_R1.0 and HP960_R1.0, except that it was made entirely of NSC with a compressive strength of 66.3 MPa. The effective depth of F0_R1.0 measured before casting was 117.5 mm [9].

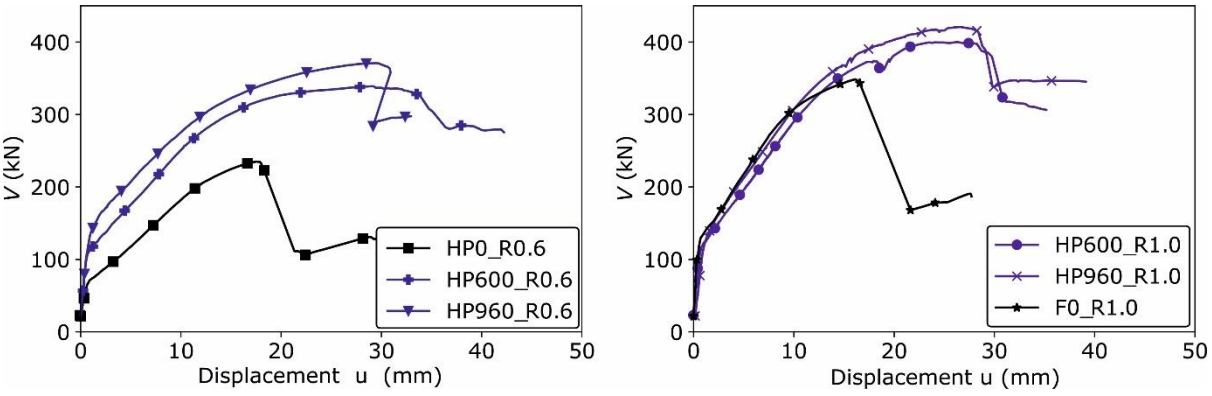

Figure 7 – Load – displacement relationships

In Figure 7, the displacement u is obtained as the relative reading between the central displacement transducer on top of the slab (D1, see Fig. 5) and the average reading of the farthest displacement transducers from the center (D2, D7, D8 and D11, see Fig. 5). The load V was obtained as the sum of measurements from the eight load cells on top of the slab, plus the self-weight of the specimen and the contributing test setup components thus, in Fig. 7, the curves start at a load level equal to the self-weight.

The main results, including maximum experimental loads V_{exp} , corresponding displacements u_{max} and failure mode are summarized in Table 4.

Table 4 – Main results (maximum load and displacement, and failure mode)

Specimen	V_{exp} (kN)	u_{max} (mm)	Failure mode
HP0_R0.6	235.0	17.6	Punching shear
HP600_R0.6	338.9	29.0	Combination of shear outside HPFRC, shear inside HPFRC and flexure
HP960_R0.6	370.9	29.2	Shear inside HPFRC (ultimately limited by punching shear at a corner of the specimen)
HP600_R1.0	399.9	26.4	Punching shear outside HPFRC zone
HP960_R1.0	420.1	26.5	One-way shear outside HFRC zone

Fig. 7 and Table 4 show that the role of HPFRC was threefold in the specimens with the lowest flexural reinforcement ratio (R0.6 specimens): it increased post-cracking stiffness, the ultimate load capacity of the specimens as well as the ultimate displacement. Referring to the specimens with flexural reinforcement ratio of 0.6%, the load capacity was increased by 44% for a 600 mm HPFRC zone width and approximately 58% for the other specimen (HP960_R0.6) with a larger HPFRC zone. The significant post-cracking stiffness means that the application of HPFRC can also be beneficial in mitigating serviceability issues in flat slabs.

Comparing the two sets of specimens, it is noticed that the differences between the reference specimen and HPFRC specimens are superior in specimens with lower flexural reinforcement ratio. For the specimens with higher reinforcement ratio, the differences in load capacity between the reference slab and the slabs with HPFRC are lower, also because F0_R1.0 (reference specimen) had a relatively high compressive strength for the conventional concrete (66.3 MPa, as mentioned earlier). In this case, the capacity of the specimens with HPFRC was increased by 15% and 21% (HP600_R1.0 and HP960_R1.0 respectively).

Referring to specimens with HPFRC with different sizes of the HPFRC zone, it is noticed that the specimens with larger HPFRC zone had a higher load capacity. However, the increase in loading capacity was small: approximately 9% in specimens R0.6 and approximately 5% in R1.0 specimens. A likely explanation of this result is the fact that flexural yielding occurred in the vicinity of the column. Also, especially in the specimens with larger area of HPFRC, flexural yielding weakened the corners of the specimens and some interaction with the test setup might have contributed to this result.

CONCLUSIONS

Five monotonic concentric punching tests were performed on flat slab specimens with varying flexural reinforcement ratio and varying extent of the zone with HPFRC in the vicinity of the column. The tests explored the possibility of enhancing the performance of composite NSC – HPFRC large scale flat slab specimens. The following main conclusions resulted from this study:

1. HPFRC with compressive strength around 125 MPa and 1% fiber volume fraction (hybrid mixture of 0.5% corresponding to triple hooked-end long fibers and 0.5% corresponding to short straight fibers) applied over at least 1.5d from the face of the column was sufficient to significantly increase the load capacity of the specimens (around 40% for specimen HP600_R0.6 compared to the reference specimen HP600_R0).

2. The use of HPFRC resulted successful in increasing the load capacity for both flexural reinforcement ratios considered in this research: 0.6% and 1.0%.

3. The use of HPFRC changed the failure mode of the specimens by pushing failure out of the HPFRC zone for the specimens with higher flexural reinforcement ratio. For lower flexural reinforcement ratio,

HPFRC was able to reduce the brittleness of the shear failure, by effectively controlling the shear crack and thereby postponing failure.

4. Besides increasing the load capacity, HPFRC delayed initial cracking of the specimens. The solution used in this paper is therefore beneficial for the Serviceability Limit State design of flat slabs, even though HPFRC was applied over only a limited region near the column support.

5. Comparing specimens with the same flexural reinforcement ratio but with different sizes of the HPFRC zone, the capacity increase was rather limited, in the range of 5% to 10% with HPFRC extending from 1.5d to 3.0d from the face of the column (meaning 2.56 times increase of HPFRC material consumption), resulting in a low cost-benefit ratio.

REFERENCES

1. Swamy RN, Ali SAR. Punching Shear Behavior of Reinforced Slab-Column Connections Made with Steel Fiber Concrete. ACI J Proc 1982;79. doi:10.14359/10917.
2. Narayanan R, Darwish IYS. Punching shear tests on steel-fibre-reinforced micro-concrete slabs. Mag Concr Res 1987;39:42–50. doi:10.1680/macr.1987.39.138.42.
3. Marzouk H, Hussein A. Experimental investigation on the behaviour of high-strength concrete slabs. ACI Struct J 1991:701–13. doi:10.14359/1261.
4. Isufi B, Pinho Ramos A. A review of tests on slab-column connections with advanced concrete materials. Structures 2021;32:849–60. doi:10.1016/j.istruc.2021.03.036.
5. Chanthabouala K, Teng S, Chandra J, Tan K-H, Ostertag CP. Punching Tests of Double-Hooked-End Fiber Reinforced Concrete Slabs. ACI Struct J 2018;115. doi:10.14359/51706891.
6. Ozden S, Ersoy U, Ozturan T. Punching shear tests of normal- and high-strength concrete flat plates. Can J Civ Eng 2006;33:1389–400. doi:10.1139/l06-089.
7. Inácio M, Lapi M, Pinho Ramos A. Punching of reinforced concrete flat slabs – Rational use of high strength concrete. Eng Struct 2020;206:110194. doi:10.1016/j.engstruct.2020.110194.
8. Hallgren M. Punching Shear Capacity of Reinforced High Strength Concrete Slabs. KTH Royal Institute of Technology, 1996.
9. Gouveia ND, Faria DM V., Ramos AP. Assessment of SFRC flat slab punching behaviour – part I: monotonic vertical loading. Mag Concr Res 2019;71:587–98. doi:10.1680/jmacr.17.00343.
10. McHarg PJ, Cook WD, Mitchell D, Yoon Y. Benefits of Concentrated Slab Reinforcement and Steel Fibers on Performance of Slab-Column Connections. ACI Struct J 2000;97:225–35.
11. Cheng M-Y, Parra-Montesinos GJ. Evaluation of Steel Fiber Reinforcement for Punching Shear Resistance in Slab-Column Connections - Part I: Monotonically Increased Load. ACI Struct J 2010;107:101–9. doi:10.14359/51663394.
12. Zohrevand P, Yang X, Jiao X, Mirmiran A. Punching Shear Enhancement of Flat Slabs with Partial Use of Ultrahigh-Performance Concrete. J Mater Civ Eng 2014;27:04014255. doi:10.1061/(asce)mt.1943-5533.0001219.
13. Nunes S, Pimentel M, Sousa C. Mechanical and fracture behaviour of an hpfrc. BEfib2021, Valencia: RILEM-fib; 2021.
14. Blazy J, Nunes S, Sousa C, Pimentel M. Development of an HPFRC for Use in Flat Slabs. RILEM Bookseries 2021;30:209–20. doi:10.1007/978-3-030-58482-5_19.
15. CEN. EN 1992-1-1. Eurocode 2 — Design of concrete structures. Part 1-1: General rules and rules for buildings. 2004.

ACKNOWLEDGEMENTS: This work was financially supported by the Fundação para a Ciência e Tecnologia – Ministério da Ciência, Tecnologia e Ensino Superior through project PTDC/ECI-EST/ 30511/2017 funded by national funds (PIDDAC). EUROMODAL, Secil, Omya Comital, Sika and Dramix are gratefully acknowledged for their collaboration and supply of materials.